Ultimate Vortex Confinement Studied by Scanning Tunneling Spectroscopy

Tristan Cren, Denis Fokin, François Debontridder, Vincent Dubost, and Dimitri Roditchev

Institut des Nanosciences de Paris, Université Pierre et Marie Curie-Paris and CNRS-UMR 7588, 4 place Jussieu, 75252 Paris, France

(Received 3 October 2008; published 27 March 2009)

We report a detailed scanning tunneling microscopy study of a superconductor in a strong vortex confinement regime. This is achieved in a thin nanoisland of Pb having a size d about 3 times the coherence length, and a thickness h such that $h \ll d \ll \lambda$, where λ is the London penetration depth. In this geometry the magnetic field evolution of local tunneling spectra reveals only two superconducting configurations to exist: zero and single vorticity. The normal state is reached at $\mu_0 H_c = 0.46$ T, about 6 times the critical field of bulk Pb, with no higher order vorticity observed. Basing on our STS data, we discuss the role of local supercurrents in both configurations.

DOI: 10.1103/PhysRevLett.102.127005 PACS numbers: 74.25.Sv, 74.25.Ha, 74.78.Na

In superconductors the macroscopic wave function evolves on the scale of the coherence length ξ while the Meissner screening is effective on the scale of the London penetration depth λ. In previous decades a lot of theoretical effort was done studying the confinement effects in superconductors of a size lower than one or both of these characteristic scales [1]. Experimentally, most of the efforts were concentrated on measuring the overall response of such systems [2–6], or to the local study of the magnetic confinement of vortices at very low magnetizing fields $H \ll H_{c2}$ on large samples $d \sim \lambda \gg \xi$ [7,8]. The organization of the vortices in real space at high fields $H \gg H_{c1}$ was reported in [9], but still at low confinement conditions, $d \gg \xi$. Very recently, penetration and expulsion of vortices in small superconducting nanostructures was studied in [10], but the detailed picture of a strongly confined superconducting state $d \sim \xi \ll \lambda_{\text{eff}}$ is still missing.

Scanning tunneling microscopy and spectroscopy (STM/STS) allows us to measure local tunneling conductance $dI/dV(V)$ revealing the quasiparticle excitation spectrum of a superconducting condensate [11]. It was experimentally observed [12] that the tunneling spectrum is affected by magnetic field and supercurrents. In the clean limit the quasiparticle excitation spectrum of current-carrying superconductor is shifted by Doppler energy [13,14], while in the diffusive limit the effect results in a finite quasiparticle lifetime due to pair breaking [14]. Recent experiments provided in both planar [15] and local STM/STS geometry [16] showed that the effect of supercurrents flowing in the superconducting sample is directly measurable by tunneling spectroscopy. In [16] it was proven that it is indeed possible to detect the supercurrents locally, the spatial resolution being limited by the extension of the superconducting wave packet [13]. Thus, the STS of confined superconductors could reveal, in addition to the gap maps, how the supercurrents are spread inside, with a resolution of the order of ξ.

In this Letter we report the local STM/STS study of the magnetic field response of a thin ($h \simeq 5.5$ nm) superconducting island having a lateral size $d \simeq 110$ nm such that $d \simeq 3\xi_{\text{eff}} \ll \lambda_{\text{eff}}$, ξ_{eff} and λ_{eff} being, respectively, the effective coherence length and the effective London penetration depth. We show that the island passes through two distinct phases that we attribute to zero vorticity ($\mu_0 H < 0.235$ T) and single vorticity ($0.235 < \mu_0 H < 0.46$ T); no higher order vorticity is observed up to the transition to the normal state at $\mu_0 H_c = 0.46$ T. The observed case corresponds to the ultimate vortex confinement: Smaller samples would not permit the vortex to exist, larger ones would allow a multiple vortex arrangement.

In contrast with previous studies of vortex confinement, our samples are impurity-free *in situ* grown crystals of Pb. The samples were prepared at room temperature by evaporation in ultrahigh vacuum (UHV) $P < 10^{-10}$ mbar of 99.99% pure Pb onto a clean 7×7 reconstructed surface of Si(111). Such a growth follows Stranski-Krastanov scenario: small well-facetted crystals of Pb are formed on a disordered wetting layer (2–3 monoatomic layers of Pb) on Si(111) [17]. This disordered interface limits the electron mean free path and thus plays an important role in the superconducting properties of the islands. The STM/STS experiments were performed *in situ* with UHV-annealed W tips at 4.3 K in magnetic fields up to 1 T. The bias voltage

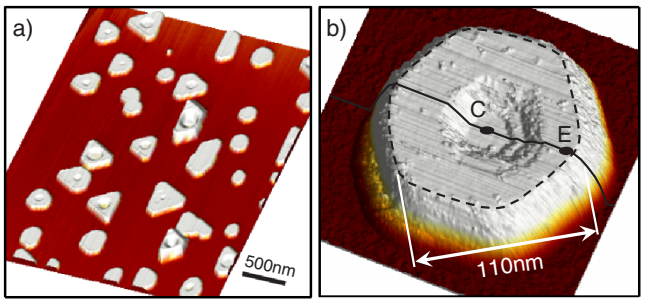

FIG. 1 (color online). Constant current topographic STM images of Pb islands on Si(111) surface taken on a large scale (a) and on a local scale (b) showing the island selected for the study. Locations C and E correspond, respectively, to the island center and edge.

was applied to the Pb islands via the metallic Pb-wetting layer.

Topographic STM images showed numerous Pb islands of different shapes with sizes varying from 50 to 500 nm [Fig. 1(a)]. We selected an isolated 19 monolayer thick island of almost ideally hexagonal shape [Fig. 1(b)] with a small thinner region in its center (13 monolayers high). To have a detailed picture of the superconducting configuration in the island at a fixed field, local $I(V)(X, Y)$ spectra were acquired at each point of the topographic image. Alternatively, $I(V)(X, H)$ data were acquired along one line crossing the island center [solid line in Fig. 1(b)], while the magnetic field was very slowly swept (1.3 mT/line). The $dI/dV(V)$ conductance spectra were normalized by the normal state background measured in a field of 0.6 T.

At zero field the tunneling conductance spectra revealed a well pronounced superconducting gap [Fig. 2(a)]. The spectra are spatially homogeneous over the whole island, even in the thinner central region: A zero-bias conductance (ZBC) of 0.26 ± 0.03 with respect to the normal state conductance was found everywhere. Such a ZBC value corresponds to the expected thermal broadening of a conventional BCS spectrum with $\Delta = 1.12 \pm 0.05$ meV. In rising magnetic field the gap in the tunneling spectra slowly fills with quasiparticle states, this effect being more pronounced on the island border where the screening supercurrents have higher density. The distribution of ZBC values has clearly radial symmetry, as the ZBC map recorded at $\mu_0 H = 0.18$ T indicates [Fig. 2(b)]. The superconducting gap is present in every location of the island; we identify this situation as the zero-vorticity state $L = 0$. In this case, the superconducting wave function $\Psi = |\Psi| e^{i\varphi}$ has a constant phase φ in London gauge, hence $\vec{\nabla}\varphi = \vec{0}$. The screening supercurrents $\vec{j}_s = -\frac{\hbar e}{m}|\Psi|^2(\vec{\nabla}\varphi + \frac{2e}{\hbar}\vec{A}) = -\frac{2e^2}{m}|\Psi|^2\vec{A}$ circulate owing to the nonzero value of the vector potential $\vec{A} = \frac{1}{2}\vec{B} \wedge \vec{r}$, where B is the magnetic field. Assuming the symmetry of revolution for the island and the fact that the magnetic field inside is almost equal to the applied field [18], we get $\vec{B} = \mu_0 \vec{H}$ and the current density $j_s = -\frac{\mu_0 e^2}{m}|\Psi|^2 rH$; i.e., it linearly increases towards the island border.

The whole dynamics of the superconducting state may be inferred from the color-coded ZBC(H, X) diagram presented in Fig. 3(a) and from selected ZBC profiles, Fig. 3(b). At zero field the ZBC is low and spatially homogeneous. As the field increases, the ZBC rises in every location of the scanned line. At each field, higher ZBC values are observed at the sample edge E as compared to the island center C, as the ZBC map in Fig. 2(b) already revealed. This smooth evolution lasts up to $\mu_0 H_0 = 0.235 \pm 0.007$ T where it is interrupted by a sudden transition [19]. At this field, the ZBC profile abruptly changes [orange or light gray curve in Fig. 3(b)]: At the island

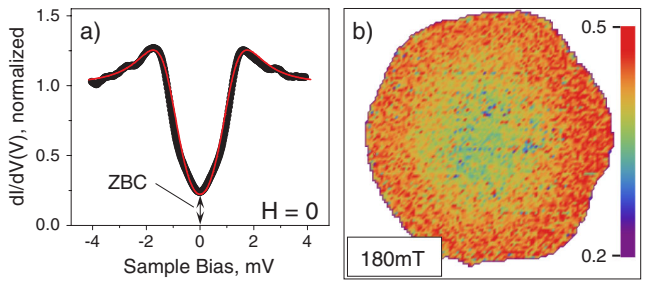

FIG. 2 (color online). (a) Characteristic local tunneling conductance spectrum $dI/dV(V)$ (set point $I_0 = 750$ pA, $V_0 = -4.5$ mV) of the island at $\mu_0 H = 0$ T (circles); best fit using standard BCS DOS with $\Delta = 1.12$ meV, $T = 4.3$ K (red or gray line). (b) In nonzero magnetic field the tunneling spectra become spatially inhomogeneous: the color-coded ZBC map of the island (here at $\mu_0 H = 180$ mT) shows the radial distribution of ZBC values with higher ZBC observed close to the island border.

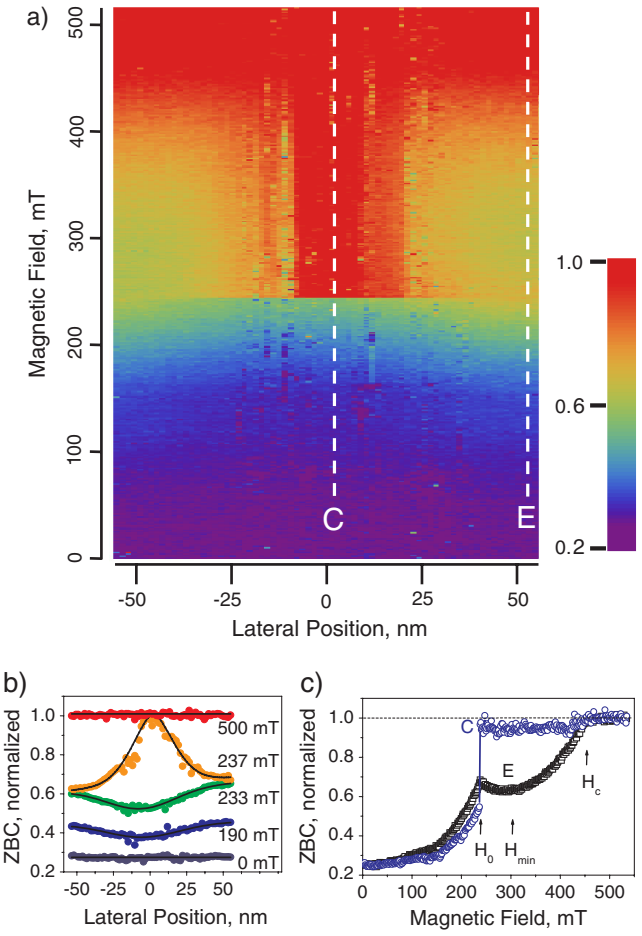

FIG. 3 (color online). (a) Color-coded diagram of ZBC values vs magnetic field taken over a line crossing the island center [solid line in Fig. 1(b)]. The abrupt transition from $L = 0$ state to $L = 1$ takes place at $\mu_0 H_0 = 235$ mT. (b) ZBC profiles: at 0 mT, in $L = 0$ configuration at 190 mT, just before the transition to $L = 1$ (233 mT), just after the transition to $L = 1$ (237 mT), in the normal state at 500 mT. (c) Evolution of the ZBC in the magnetic field in locations C (blue or dark gray circles) and in E (black circles).

center it becomes ~1; i.e., it takes the normal state value [curve C in Fig. 3(c)]. At the sample border E, however, the ZBC does not change significantly [curve E in Fig. 3(c)]. The reproducibility of the transition field was confirmed by four full successive STS runs in rising and lowering fields.

To dress a detailed picture of the transition, we present in Fig. 4 the evolution of the local tunneling conductance spectra $dI(V)/dV$ taken in the positions C and E. In the location C the gap in the local tunneling spectra disappears at H_0 [Fig. 4(a)], indicating an abrupt destruction of the superconducting order in the island center due to the vortex entry. At the same time, the superconducting gap does not close at the sample border E [Fig. 4(b)]. Such behavior suggests that the island has transited into a single-vorticity state $L = 1$ in which the superconducting wave function has a phase gradient $|\vec{\nabla}\varphi| = 1/r$. Remarkably, in the field range $0.235\ \mathrm{T} < \mu_0 H < 0.36\ \mathrm{T}$ the superconducting gap at the island border appears even more pronounced than at the transition at H_0 [curve E in Fig. 3(c)]. At higher fields the island undergoes a smooth transition to the normal state characterized by continuous gap filling with increasing field, up to $\mu_0 H_c = 0.46$ T at which the gap in the local tunneling spectra totally disappears (Figs. 3 and 4).

To understand in detail the observed dynamics in tunneling spectra, it is essential to remind the existence of the disordered interface between the island and Si(111) substrate, due to the amorphous wetting layer [17] that limits the quasiparticle mean free path to $l \approx 2h = 11$ nm. The coherence length and the penetration depth for such a thin and diffusive superconductor take the effective values: $\xi_{\mathrm{eff}} \simeq 0.85\sqrt{\frac{\xi_0 l}{1-T/T_c}}$ and $\lambda_{\mathrm{eff}} \simeq \lambda^2/h$ with $\lambda \simeq 0.64\lambda_0\sqrt{\frac{\xi_0}{l(1-T/T_c)}}$ where $\xi_0 = 80$ nm and $\lambda_0 \simeq 50$ nm are, respectively, the coherence length and the penetration depth in bulk Pb [20]. Considering the island geometry we get $\xi_{\mathrm{eff}} \simeq 40$ nm and $\lambda_{\mathrm{eff}} \simeq 4\ \mu$m at $T = 4.3$ K. Thus, the situation in the island, $l \ll \xi_{\mathrm{eff}} \ll \lambda_{\mathrm{eff}}$, is similar to that of a type II superconductor in the diffusive limit. The condition $h \ll d \ll \lambda_{\mathrm{eff}}$ implies that, although strong screening supercurrents may circulate in the island, their diamagnetic (Meissner) effect is weak; i.e., the external magnetic field almost fully penetrates the sample, within <1% [18].

As the field is applied, the screening supercurrents start flowing [Fig. 5(a)], modifying the local tunneling spectra. According to Maki [14] the effects of supercurrents may be described by a pair-breaking parameter Γ that broadens the quasiparticle excitation spectrum [15]. At the intermediate temperature of our experiment $T \approx 0.6T_c$ [21] the thermal smearing of the broadened quasiparticle spectrum results in an enhancement of the ZBC in the $dI/dV(V)$ tunneling data. Thus, the ZBC value in the tunneling spectra is a good indicator of the current density. In $L = 0$ state, we indeed observed the increase of the ZBC, with larger values at the sample border [Figs. 2(b) and 3]. For a quantitative analysis, however, one has to take into account spatial convolution effects over an area $\sim\xi_{\mathrm{eff}}^2$ [13,14].

We now discuss in more detail the transition at $\mu_0 H_0 = 0.235$ T. The normal region appearing at $H \geq H_0$ in the center C may be clearly identified: Its small size $\sim 2\xi_{\mathrm{eff}}$ and corresponding bell-shaped spatial ZBC profile [orange or gray curve in Fig. 3(b)] are two well-recognized features of a vortex core [22]. At the sample border E, however, the rapid dynamics of the ZBC below H_0 towards the normal state is somehow delayed due to the appearance of the vortex [Fig. 3(c)], allowing the superconductivity to sur-

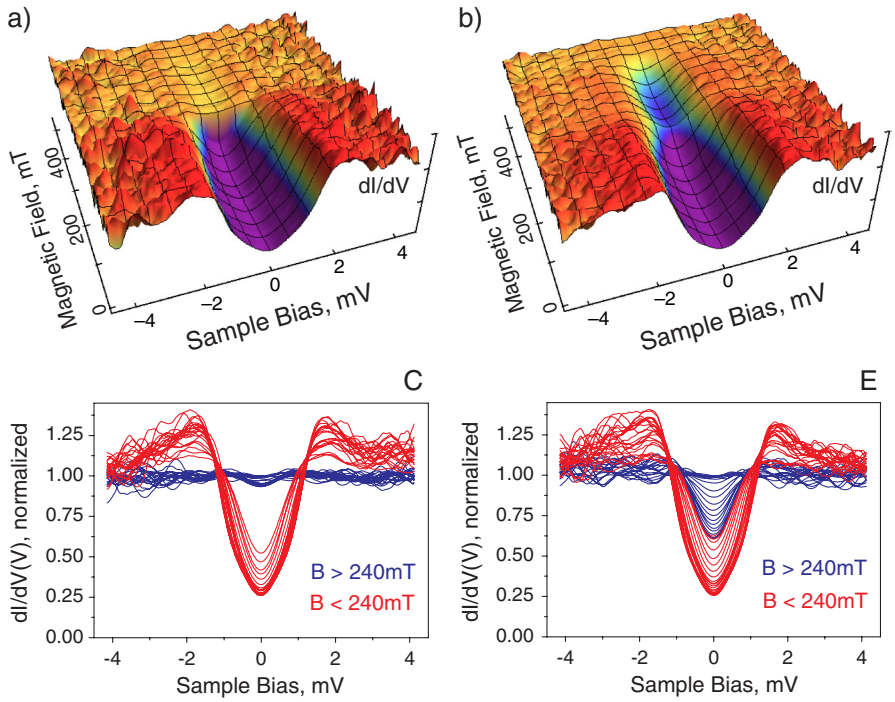

FIG. 4 (color online). Evolution of the local tunneling $dI/dV(V)$ spectra (set point $I_0 = 750$ pA, $V_0 = -4.5$ mV) in the magnetic field. (a) In the island center, at the location C [see Fig. 1(b)]; (b) At the sample border, location E. Each data set is presented as 2D and 3D plots for clarity.

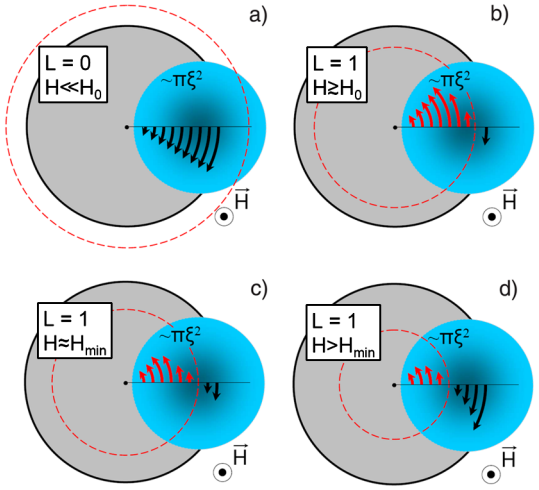

FIG. 5 (color online). Tentative picture of the superfluid velocity v_s distribution over the island (gray disc) at low fields (a), at H_0 just after transition into $L = 1$ state (b), at $H_{\min}$ (c), and at $H_{\min} < H < H_c$ (d). Black arrows represent Meissner screening currents, red or gray arrows—vortex-generated currents. Dashed line contour delimits the surface penetrated by the flux quantum ϕ_0. The blue or medium gray circle $\pi\xi_{\text{eff}}^2$ centered near the sample border shows the superconducting wave packet extension [13].

vive up to higher fields. At H_0 the total kinetic energy of the screening supercurrents in $L = 0$ configuration $E_c(L = 0)$ becomes equal to the sum of the kinetic energy of currents in $L = 1$ configuration $E_c(L = 1)$ and the condensation energy of the vortex core E_{cond}. In $L = 1$ configuration the total current drops significantly due to the partial compensation of Meissner screening currents by the vortex-generated supercurrents, making single-vorticity energetically favorable [Fig. 5(b)]. Thus, the phenomenon is similar to the Little-Parks effect but taking place at $\phi = 1.3 \pm 0.1\phi_0$, depending on the considered area of the sample, and not at $\phi_0/2$ [23], where $\phi_0 = h/2e$.

As the field further increases, the normal state at the island center C remains [curve C in Fig. 3(c)]. At the sample periphery, however, the tunneling spectra reveal an interesting nonmontonic evolution: after the transition to $L = 1$ the ZBC starts to decrease with increasing field, reaching a local minimum at $H_{\min} \simeq 0.3$ T [curve E in Fig. 3(c), 3D plot in Fig. 4(b)]. In fact, in $L = 1$ configuration the total current may be seen as a superposition of vortex-generated supercurrents and screening Meissner supercurrents circulating in the opposite direction. Just after the transition the vortex currents dominate the total current [Fig. 5(b)]. In higher fields the Meissner component increases, and a partial compensation between Meissner and vortex currents occurs near the island border [24]. This partial compensation [Fig. 5(c)] leads to the diminution of the pair-breaking effects [14] and thus, to the reduction of ZBC. Note that such a reentrant effect was not reported in [10], probably due to the limited resolution in the ZBC(H) data.

The simple analysis of the observed tunneling spectra allows us to dress a consistent picture of the magnetic field response of a thin superconducting island of size $d \sim 3\xi_{\text{eff}}$. At low fields a zero-vorticity state is the lowest energy configuration. At higher fields, however, a single-vorticity configuration $L = 1$ becomes energetically favorable: the transition takes place at $\phi = 1.3 \pm 0.1\phi_0$. The double-vorticity state is not reached in this island; a slightly larger island would accept $L = 2$ configuration to appear. Thus, the studied superconducting system represents the ultimate case where only $L = 0$ and $L = 1$ vorticities are possible.

[1] See, for example, V. V. Moshchalkov, X. G. Qiu, and V. Bruyndoncx, Phys. Rev. B **55**, 11 793 (1997); V. A. Schweigert, F. M. Peeters, and P. S. Deo, Phys. Rev. Lett. **81**, 2783 (1998); A. S. Mel'nikov, D. A. Ryzhov, and M. A. Silaev, Phys. Rev. B **78**, 064513 (2008), and references therein.
[2] W. A. Little and R. D. Parks, Phys. Rev. Lett. **9**, 9 (1962).
[3] G. Boato *et al.*, Solid State Commun. **3**, 173 (1965).
[4] V. V. Moshchalkov *et al.*, Nature (London) **373**, 319 (1995).
[5] A. Kanda *et al.*, Phys. Rev. Lett. **93**, 257002 (2004).
[6] T. Nishio *et al.*, Appl. Phys. Lett. **88**, 113115 (2006).
[7] T. Nishio *et al.* Phys. Rev. B **77**, 012502 (2008).
[8] S. Okayasu *et al.*, IEEE Trans. Appl. Supercond. **15**, 696 (2005).
[9] G. Karapetrov *et al.*, Phys. Rev. Lett. **95**, 167002 (2005); M. Iavarone *et al.*, Physica (Amsterdam) **460C–462C**, 952 (2007).
[10] T. Nishio *et al.*, Phys. Rev. Lett. **101**, 167001 (2008).
[11] I. Giaever and K. Megerle, Phys. Rev. **122**, 1101 (1961).
[12] J. L. Levine, Phys. Rev. **155**, 373 (1967).
[13] P. G. de Gennes, *Superconductivity of Metals and Alloys* (W. A. Benjamin, Inc., New York, 1966).
[14] K. Maki and P. Fulde, Phys. Rev. **140**, A1586 (1965); for a review, see also K. Maki in *Superconductivity*, edited by R. D. Parks (Marcel Dekker, New York, 1969).
[15] A. Anthore, H. Pothier, and D. Esteve Phys. Rev. Lett. **90**, 127001 (2003).
[16] A. Kohen *et al.*, Phys. Rev. Lett. **97**, 027001 (2006).
[17] M. C. Hupalo *et al.*, Surf. Sci. **493**, 526 (2001); K. Budde *et al.*, Phys. Rev. B **61**, R10602 (2000).
[18] E. H. Brandt and J. R. Clem, Phys. Rev. B **69**, 184509 (2004).
[19] For all observed events we did not find any hysteretic behavior in the magnetic field within 3% of the experimental error.
[20] M. Tinkham, Phys. Rev. **129**, 2413 (1963).
[21] D. Eom *et al.*, Phys. Rev. Lett. **96**, 027005 (2006).
[22] H. F. Hess *et al.*, Phys. Rev. Lett. **62**, 214 (1989).
[23] V. A. Schweigert and F. M. Peeters, Phys. Rev. B **57**, 13817 (1998); **60**, 3084 (1999); L. F. Chibotaru *et al.*, Nature (London) **408**, 833 (2000).
[24] This compensation cannot be complete, however, since these components have different radial dependencies; the effect of compensation on ZBC depends on $\langle v_s^2 \rangle$ with spatial averaging over $\sim \xi^2$.